Stochastic Generation of Regular Distributions

Abstract. *A new class of models is proposed to describe the dynamic processes leading to the establishment of regular spatial patterns of structures in natural systems. Simple mathematical arguments are used to compute the saturating densities of the distributions, and these results are verified by computer simulation of model systems.*

A regular spatial distribution of structures can be generated by a process of random structure initiation followed by locally spreading inhibition which prevents new structure formation in an ever widening region around each structure once it has formed. Despite the widespread occurrence of regular distributions, and their importance in such diverse fields as metallurgy (*1*), cell biology (*2*), developmental biology (*3*), ecology (*4*), and geography (*5*), model systems in which there is an interval, due to such processes as growth or transport, between the time when the structure is formed and the time when the surrounding inhibitory field is established have not been carefully studied. Here, I compute the saturating densities for systems of random structure initiation in which inhibitory fields are transmitted either with a linear velocity or by diffusion transport.

Consider a one-dimensional, initially homogeneous system of length L, in which no structures are present, but in which random fluctuations, localized in space, of sufficient magnitude to initiate structure formation, are occurring at a rate $F(l^{-1}t^{-1})$, where the symbols in parentheses indicate that the rate is inversely proportional to length and time. Once a structure is formed, it remains localized and inhibits completely new structure formation at all points lying closer than a distance $s = |v(t - t_0)|$, where t_0 is the time of formation of the structure and $v(lt^{-1})$ is the velocity of spreading of the inhibitory field. New structure formation proceeds outside the inhibitory fields of established structures at the rate F. At any time the number of structures is designated N, the density $n = N/L$, and the length available for new structure formation ϕL. The density when new structure formation ceases, $n^* = N^*/L$, is called the saturation density. If we consider the limit $L \to \infty$, and average over a large number of trials to an initially homogeneous system at fixed F and v, the values of the dynamic variables, n and ϕ, will be centered around single most probable values as a function of time, and equations giving the interdependence of these average variables can be derived (*6*).

The rate at which new structures are formed is proportional to the available length in which no inhibitory fields are present, so that the density increase is given by

$$\frac{dn}{dt} = F\phi \tag{1}$$

For low densities, at which the inhibitory fields of neighboring structures do not overlap, ϕ will decrease at the rate $2nv$. As the density nears the saturating density, and neighboring fields begin to overlap, the rate of decrease of ϕ diminishes. This decrease may be described by a monotonically decreasing function $g(n/n^*)$ which depends only on the ratio (n/n^*), such that

$$\frac{d\phi}{dt} = -2nvg \tag{2}$$

where

$$g(0) = 1 \qquad g(1) = 0 \tag{3}$$

Equations 1 and 2 can be combined to form the single differential equation

$$\frac{dn}{d\phi} = \frac{-F\phi}{2nvg} \tag{4}$$

which can be immediately integrated, subject to the boundary conditions

$$\begin{aligned} n(1) &= 0 \qquad \phi(0) = 1 \\ n(0) &= n^* \qquad \phi(n^*) = 0 \end{aligned} \tag{5}$$

to give

$$n^* = k\left(\frac{F}{v}\right)^{1/2} \tag{6}$$

where k is a constant depending on the function g. Since g is equal to unity for a wide range of low densities, but decreases rapidly to zero as the density approaches the saturation density, we assume it can be approximated by the expression,

$$g = 1 - \left(\frac{n}{n^*}\right)^m \tag{7}$$

where we anticipate that m will be larger than 1. When Eq. 7 is substituted in Eq. 4, and the integrations are performed, we find

$$k = \left(\frac{m+2}{2m}\right)^{1/2} \tag{8}$$

Provided m is larger than 1, effective limits $0.707 < k < 1.225$ can be placed on k.

The simple functional dependence displayed in Eq. 6 can be confirmed from a dimensional analysis of the model system. Consider a system of physical dimension d and volume $V(l^d)$, in which fluctuations are occurring at a rate $F(l^{-d}t^{-1})$ and the inhibitory field spreads at a velocity $v(lt^{-1})$. Since N^* is a dimensionless number, the principle of dimensional homogeneity requires that it must be some function of dimensionless variables (*7*). The model system under consideration is completely specified by three variables, F, v, and V and there is only one way these variables can be combined to make a dimensionless number. This number, designated K, is given by

$$K = \left(\frac{F}{v}\right)^{\frac{d}{d+1}} V \tag{9}$$

so that

$$N^* = f(K) \tag{10}$$

Now, as the volume increases at constant F and v, the number density per unit volume will converge to some constant value, and consequently for both N^* and V large, N^* must display a linear dependence on V. This, in conjunction with Eq. 10, uniquely determines N^*,

$$N^* = k_d\left(\frac{F}{v}\right)^{\frac{d}{d+1}} V \tag{11}$$

where k_d is a constant depending on the dimension of the system. Equation 6 follows at once for $d = 1$.

A computer simulation was devised to empirically test Eq. 6. Consider a one-dimensional system for which F, v, and L have been specified. The length is subdivided into M compartments of length Δx, and a time iteration Δt is then determined, so that

$$M\Delta x = L \qquad \Delta t = \frac{\Delta x}{v} \tag{12}$$

The number of structure forming fluctuations, initially occurring in the whole system in time Δt, is $FL\Delta t$. Provided the number of compartments is very much larger than the number of fluctuations in Δt, the probability p of having a single structure formed in any one compartment in time Δt is

$$p = \frac{FL\Delta t}{M} = F\Delta x\Delta t \ll 1 \tag{13}$$

and the probability of having two structures formed in a compartment will be

negligible. The iteration length, Δx, must be chosen sufficiently small that the inequality in Eq. 13 is satisfied. An initially empty system of M compartments is then considered. For each compartment, for each time iteration, a random number $0 \leq r \leq 1$ is generated. If $r \leq p$ in a compartment, a new structure is formed in that compartment; if $r > p$ nothing happens. Once a structure is formed it acts as a center of an inhibitory field which moves outward one new compartment at each time iteration. At subsequent time iterations, in compartments in which there is neither a structure nor an inhibitory field, random structure initiation proceeds as before. Substituting Eqs. 8, 12, and 13 into Eq. 6, we find the expected number of structures for this discrete representation of the continuous system

$$N^* = \left(\frac{(m+2)\,p}{2m}\right)^{1/2} M \qquad (14)$$

In Fig. 1 we display the average number of structures formed over 40 trials to systems of 1000 and 2000 compartments. The straight line, a least squares fit to a linear equation, has a value of 1.85 for the y intercept and a slope of 0.830 (this gives m in Eq. 14 equal to 5.3), with a standard error of the estimate equal to 1.22. The deviation from zero at the origin arises because Eq. 14 is valid only where both N^* and M are large. As the right-hand side of Eq. 14 becomes smaller than one, the expected interparticle spacing becomes greater than the length of the system. However, if the right-hand side of Eq. 14 remains greater than zero, a single structure must always be formed, leading to a finite discontinuity at the origin in Fig. 1.

In Fig. 2 we display two measures which can be used to characterize deviations from randomness: the variation of the expected number of structures around N^* (Fig. 2a), and the pair correlation function (the number density at distance R from a structure divided by the mean number density) (Fig. 2b). We compare these measures for the model system with $p = .02$ and $M = 100$ ($N^* = 12.1$) with the theoretical values for a random system of 100 compartments, which is generated by assuming that the probability of having a structure in each compartment is independent of occupation of neighboring compartments, and is equal to $N^*/100 = .121$. In the model system there is a striking sharpening of the distribution (standard deviation 2.06

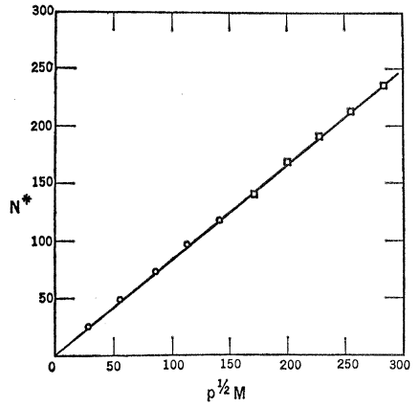

Fig. 1. Mean number of structures formed as a function of $p^{1/2}M$ for the model system described in the text. Each point represents an average of 40 trials to systems with $M = 1000$ (circles) and $M = 2000$ (squares). The straight line is a least squares fit to a linear equation.

compared with a theoretical 3.25 for the binomial distribution). There is also strong local inhibition of structures in the immediate region surrounding a structure already formed, although subsidiary peaks in the correlation function, such as are found in liquids, are not present.

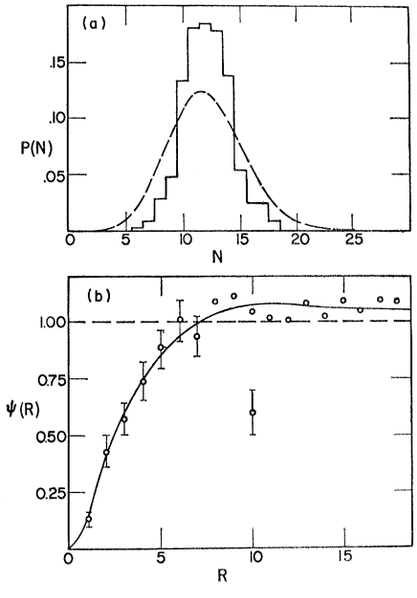

Fig. 2. Comparison of measures used to characterize deviations from randomness for the model system averaged over 300 trials with $p = .02$ and $M = 100$ (solid line), and the theoretical values for a randomly generated system at the same average density (dashed line). (a) The probability distribution, $P(N)$, as a function of N. The theoretical curve is the binomial distribution. (b) The pair correlation function, $\psi(R)$, as a function of R. The 95 percent confidence limits for most of the points is indicated in the center of the figure. The values of $\psi(R)$ near the origin have a smaller variance and the confidence limits have been indicated.

The technique of dimensional analysis, used to confirm Eq. 6, can be readily extended to predict the functional dependence of N^* for cases in which the inhibitory field follows different dynamics. For example, if random fluctuations occur as above, but the inhibitory field is transmitted by a substance which diffuses with diffusion coefficient $D(l^2t^{-1})$ and inhibits completely new structure formation if it is present at a concentration greater than a predetermined threshold, the expected number of structures will be

$$N^* = k_d' \left(\frac{F}{D}\right)^{\frac{d}{d+2}} V \qquad (15)$$

a result which has also been confirmed by computer simulation for $d = 1$ (*8*).

The models discussed here must be distinguished from the better studied, mathematically simpler systems in which an initially homogeneous system becomes everywhere unstable with respect to infinitesimal fluctuations of finite wavelength (*9*). The latter systems will be expected to give a more regular distribution of structures than those encountered here, but this difference in regularity cannot be quantitatively characterized at present (*10*). The models under consideration more closely correspond to systems in which there is random sequential addition of structures of fixed size to an initially homogeneous field. Although there is a rich theoretical literature analyzing these systems (*6, 11*), these models do not represent the dynamic properties of the inhibitory fields. A comparison of the naturally occurring distributions of structures and the distributions resulting from theoretical models should be useful in characterizing the dynamic processes leading to the regular distributions found in nature.

LEON GLASS

Institute for Fundamental Studies, Department of Physics and Astronomy, University of Rochester, Rochester, New York 14627

References and Notes

1. B. Chalmers, *Principles of Solidification* (Wiley, New York, 1964); R. J. Gerdes, A. T. Chapman, G. W. Clark, *Science* **167**, 979 (1970).
2. P. Weiss, *Proc. Nat. Acad. Sci. U.S.A.* **68**, 846 (1971); G. G. Maul, J. W. Price, M. L. Lieberman, *J. Cell Biol.* **51**, 405 (1971).
3. V. B. Wigglesworth, *J. Exp. Biol.* **17**, 180 (1940); P. A. Lawrence and P. Hayward, *J. Cell Sci.* **8**, 513 (1971); H. Ursprung, in *Major Problems in Developmental Biology*, M. Locke, Ed. (Academic Press, New York, 1966), p. 177.

4. E. C. Pielou, *J. Ecol.* **48**, 575 (1960); *An Introduction to Mathematical Ecology* (Wiley, New York, 1969).
5. W. Christaller, *Central Places in Southern Germany* (Prentice-Hall, Englewood Cliffs, N.J., 1966); L. Glass and W. Tobler, *Nature* **233**, 67 (1971).
6. B. Widom [*J. Chem. Phys.* **44**, 388 (1966)] gives a more detailed discussion of the approach to the thermodynamic limit for the related problem of random sequential addition of hard spheres to a homogeneous field.
7. W. J. Duncan, *Physical Similarity and Dimensional Analysis* (Arnold, London, 1953).
8. L. Glass, in preparation.
9. Linear stability theory has been applied to study regular pattern formation in physics and biology → A. M. Turing, *Phil. Trans. Roy. Soc. London Ser. B* **237**, 37 (195→ J. W. Cahn, *J. Chem. Phys.* **42**, 93 (1965); I. Prigogine and G. Nicolis, *Quart. Rev. Biophys.* **4**, 107 (1971).
10. Qualitative discussions of the differences can be found in K. C. Sondhi, *Quart. Rev. Biol.* **38**, 289 (1963); J. W. Cahn and R. J. Charles, *Phys. Chem. Glasses* **6**, 181 (1965).
11. B. E. Blaisdell and H. Solomon, *J. Appl. Probab.* **7**, 667 (1970).
12. Partially supported by NSF grant GU-4040.

8 January 1973

Apollo 17 Seismic Profiling: Probing the Lunar Crust

Abstract. *Apollo 17 seismic data are interpreted to determine the structure of the lunar crust to a depth of several kilometers. Seismic velocity increases in a marked stepwise manner beneath the Taurus-Littrow region at the Apollo 17 site. A thickness of about 1200 meters is indicated for the infilling mare basalts at Taurus-Littrow. The apparent velocity is high (about 4 kilometers per second) in the material immediately underlying the basalts.*

The successful installation of a geophysical station at the Taurus-Littrow landing site of the Apollo 17 mission marked the culmination of an exciting period of manned lunar exploration and vastly improved our knowledge of the lunar interior. Before the Apollo 17 mission there was a surprising gap in our knowledge concerning the nature of the upper 10 km of the lunar crust because of the absence of pertinent seismic travel time data at distances closer than 30 km. Travel times of seismic waves are inverted to determine the seismic velocity structure and provide the direct means of probing the lunar interior.

The seismic velocity in the moon was known to increase rapidly from values of 100 to 300 m/sec in the upper 100 m to a value of about 6 km/sec at a depth of 15 to 20 km. Even though the seismic velocity variation was believed to be a smooth increase with depth it was surmised (*1*) that such a rapid increase of velocity (approximately 2 km/sec per kilometer) could not be explained solely by the effect of increasing pressure on dry rocks with macroscopic and microscopic cracks or by the self-compression of any granular rock powder.

Laboratory velocity measurements on returned lunar soils and on terrestrial sands and basaltic ash (*2*) have indicated velocity-depth gradients of 0.4 to 0.8 km/sec per kilometer, but such gradients occur only to pressures of about 50 bars (corresponding to a lunar depth of about 1 km). An examination of these experimental data led to the inference that compositional or textural changes must be important in the upper 5 km of the moon (*1*).

The purpose of the Apollo 17 lunar seismic profiling experiment was to record on a triangular array of four seismometers the vibrations of the lunar surface as induced by explosive charges, the thrust of the lunar module (LM) ascent engine, and the crash of the LM ascent stage.

Strong seismic signals were recorded from the detonation of eight explosive charges, which were armed and placed on the lunar surface by the Apollo 17 crew at various points along the traverses. The weights of the explosive charges ranged from 0.06 to 2.7 kg. Recording of these signals generated seismic travel time data in the distance range from 0.1 to 2.7 km.

One of the more significant events of the Apollo 17 mission was the recording of the seismic signal from the LM ascent stage, which struck the lunar surface 8.7 km southwest of the landing site in the highlands of the South Massif. The seismic signals from this impact were observed at a greater depth of penetration than could be achieved solely with the use of small explosive charges. The impact signal was similar in character to previous impact signals, having an emergent beginning and a long duration (*3*, *4*).

The observed travel times for the detonation of the explosive charges can be combined with the observed travel time for the LM impact to provide information about the seismic velocity to a depth of several kilometers beneath the Apollo 17 landing site. Since the LM impacted at an elevation of 1.2 km above the recording seismometer array the LM travel time has been adjusted to the same reference elevation as the geophone array. The correction is small and decreases the observed time of 5.75 seconds by 0.18 second. Travel time data from the LM impact and the explosive charges are plotted against distance in Fig. 1. Three *P*-wave (compressional wave) velocities are represented in the travel time data: 250, 1200, and 4000 m/sec. There is some uncertainty in the apparent velocity of 4000 m/sec determined primarily by the LM impact data point at a distance

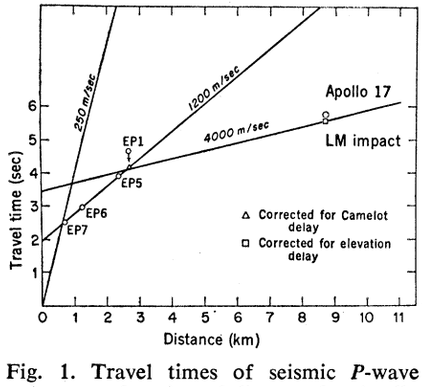

Fig. 1. Travel times of seismic *P*-wave pulses as a function of distance for Apollo 17 explosive charges and the LM impact. The data points defining the 250-m/sec line are omitted for brevity. The travel time for explosive package 1 (EP1) was corrected for propagation delay through a large crater, Camelot, and the LM impact travel time was corrected for an elevation effect.

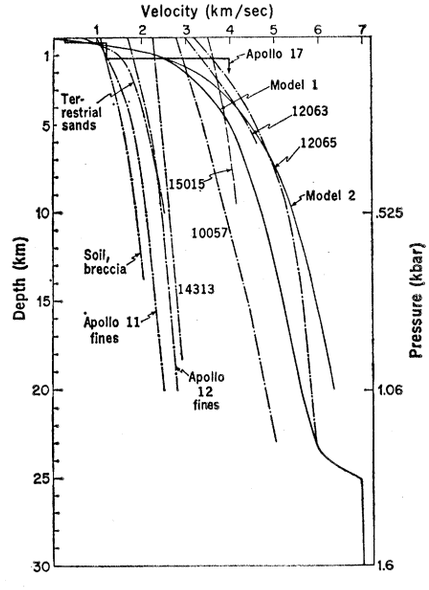

Fig. 2. Velocity model from the Apollo 17 results compared to earlier lunar models [models 1 and 2 (*4*)] and to velocities for lunar rocks and terrestrial sands measured in the laboratory as a function of pressure. Lunar rocks are identified by sample numbers.